

X-ray fluorescence microscopy of light elements in cells: self-absorption correction by integration of compositional and morphological measurements

This content has been downloaded from IOPscience. Please scroll down to see the full text.

2013 J. Phys.: Conf. Ser. 463 012022

(<http://iopscience.iop.org/1742-6596/463/1/012022>)

View [the table of contents for this issue](#), or go to the [journal homepage](#) for more

Download details:

IP Address: 80.82.78.170

This content was downloaded on 10/01/2017 at 18:48

Please note that [terms and conditions apply](#).

You may also be interested in:

[Absolute zinc quantification at the sub-cellular level by combined use of hard X-ray fluorescence and phase contrast imaging techniques](#)

Ewelina Kosior, Sylvain Bohic, Heikki Suhonen et al.

[Correlative Imaging of Structural and Elemental Composition of Bacterial Biofilms](#)

Y Yang, R Heine, F Xu et al.

[Recent developments at the TwinMic beamline at ELETTRA: an 8 SDD detector setup for low energy X-ray Fluorescence](#)

A Gianoncelli, G Kourousias, A Stolfa et al.

[Development of fast parallel multi-technique scanning X-ray imaging at Synchrotron Soleil](#)

K Medjoubi, N Leclercq, F Langlois et al.

[Construction of the Scanning Transmission X-ray Microscope Beamline at UVSOR](#)

T Ohigashi, H Arai, T Araki et al.

[Low-dose phase-contrast X-ray imaging: a comparison of two methods](#)

T Zhou, U Lundström, D H Larsson et al.

[New Developments in Hard X-ray Fluorescence Microscopy for In-situ Investigations of Trace Element Distributions in Aqueous Systems of Soil Colloids](#)

Sophie-Charlotte Gleber, Britta Weinhausen, Sarah Köster et al.

[New Energy Sources: in-situ Characterisation of Fuel Cell and Supercapacitor Components.](#)

[Complementary Studies using Transmission, Fluorescence and Photoelectron Microscopy and Imaging](#)

B Bozzini, M Amati, A Gianoncelli et al.

X-ray fluorescence microscopy of light elements in cells: self-absorption correction by integration of compositional and morphological measurements

E Malucelli¹, S Iotti^{1,2}, M Fratini^{3,8}, C Marraccini⁹, A Notargiacomo³, A Gianoncelli⁴, I Bukreeva³, A Cedola³, J Maier⁵, G Farruggia^{1,2}, C Cappadone¹, L Merolle¹, F Wolf⁶, V Trapani⁶ and S Lagomarsino⁷

¹ Dipartimento di Farmacia e Biotecnologie, Univ. di Bologna, It

² Istituto Nazionale Biostrutture e Biosistemi, Rome, It

³ Institute of Photonics and Nanotechnology - CNR, Rome, It

⁴ Sincrotrone Trieste, Area Science Park, Basovizza Trieste, It

⁵ Dipartimento di Scienze Bionediche e Cliniche L. Sacco, Univ. di Milano, Milan, It

⁶ Istituto Patologia Generale, Univ. Cattolica del Sacro Cuore, Rome, It

⁷ Institute Chemical and Physical processes, c/o Phys. Dpt. Univ. Sapienza, Rome, It

⁸ Fermi Center, Piazzale del Viminale 1 00187 Roma

⁹ Dipartimento di Scienze della Vita, Univ. di Modena e Reggio Emilia, Modena, It

E-mail: stefano.lagomarsino@cnr.it

Abstract. We present here a new methodology for quantitative mapping of light elements in cells, based on combination of compositional and morphological information, derived respectively by X-ray Fluorescence Microscopy (XRFM), Atomic Force Microscopy and Scanning Transmission X-ray Microscopy (STXM). Since XRFM of light elements (carbon, nitrogen, oxygen, sodium and magnesium), are strongly influenced by self-absorption, we developed an algorithm to correct for this effect, using the morphological and structural information provided by AFM and STXM. Finally, the corrected distributions have been obtained, thus allowing quantitative mapping.

1. Introduction

X-ray Fluorescence Microscopy (XRFM) is a powerful method to measure elemental content and distribution in many kind of materials. In recent years considerable attention has been given to application of XRFM in cell biology, in particular for its ability to map trace elements in cells [1, 2]. Fluorescence micro-tomography has been also applied to diatoms for quantitative determination of element distribution in 3D [3]. In a recent paper [4] we have demonstrated that it is possible to merge compositional and morphological information to quantitatively derive the element concentration (magnesium in that case) combining XRFM with Atomic Force Microscopy (AFM). In this paper we aim to demonstrate that morphological data derived by AFM and by Scanning Transmission X-ray Microscopy (STXM) are crucial for mapping also main cell components, i.e. carbon (C), nitrogen (N) and oxygen (O), whose fluorescence radiation is strongly affected by the absorption in the cell itself (self-absorption effect). We therefore developed a specific algorithm to correct for self-absorption, and applied this procedure to obtain the true element distribution C, N, O, Na and Mg.



2. Experimental and results

2.1. Sample preparation

A colon carcinoma cell line (LoVo) was used in this study. The cells were cultured in RPMI medium (Sigma) supplemented with 10% PBS (phosphate buffered saline), 2 mM glutamine, 100 U/ml penicillin, and 100 µg/ml streptomycin sulphate. At 50-80% confluency, the cells were briefly rinsed in 150 mM KCl, then fixed in ice-cold methanol/acetone 1:1 and air dried.

2.2. XRFM and AFM measurements

The XRFM measurements on LoVo cells were carried out using synchrotron radiation at the TWINMIC beamline at ELETTRA. Fresnel zone plate lenses were used to focalize the incoming 1.5 keV beam, monochromatized by grating monochromators. The final spot size onto the sample was evaluated to be around 500 nm. The samples were transversally scanned in the zone plate focus, and at each scan step eight full fluorescence spectra were simultaneously acquired by 8 Si-drift detectors (SDD) placed radially with respect to the sample. The angle formed by the SDDs and the sample plane was 20° [5]. The SDDs have a 30mm² active area and certified >90% sensitivity for the photon energy range 200–15000 eV [6]. The flux transmitted (T) by the sample was simultaneously measured with a CCD camera. Zone plate, sample and detectors were in vacuum, thus avoiding any absorption by air. AFM topography maps were collected off-line by a Digital Instruments D3100 AFM equipped with a Nanoscope IIIa controller. The AFM was operated in air ambient using Tapping Mode at a resonance frequency of about 260 kHz. Commercial monolithic silicon tips were employed, with an apex curvature radius in the 5-10 nm range and a nominal force constant of 40 N m⁻¹. The scan size used was 55 µm and the image resolution in pixels was 512x512. Images were collected without any real-time filtering or flattening, and were post-processed to eliminate all the possible artifacts [4].

2.3. Fluorescence spectra analysis

The fluorescence spectra were analyzed for each scan step with the program PyMCA [7], and deconvoluted into their components, considering the incident photon energy of about 1.5 keV. Under these conditions C, N, O, Na, Mg were detected in LoVo cells. The resulting fluorescence intensity maps provided information on the total elemental content in the volume illuminated by the beam at each scanning step. However, especially for the lightest elements, the fluorescence radiation experiences strong self-absorption due to penetration in the sample itself. Figure 1 shows the raw oxygen fluorescence maps of four of the eight detectors, whose position with respect to the sample is schematically indicated in the figure. The intensity inhomogeneity due to self-absorption is clearly detected. Indeed the sides of raw maps opposite to the detectors show low intensity due to the self-absorption, while the sides close to the detectors show high intensity. In the figure the color scale goes from blue (low intensity) to red (high intensity).

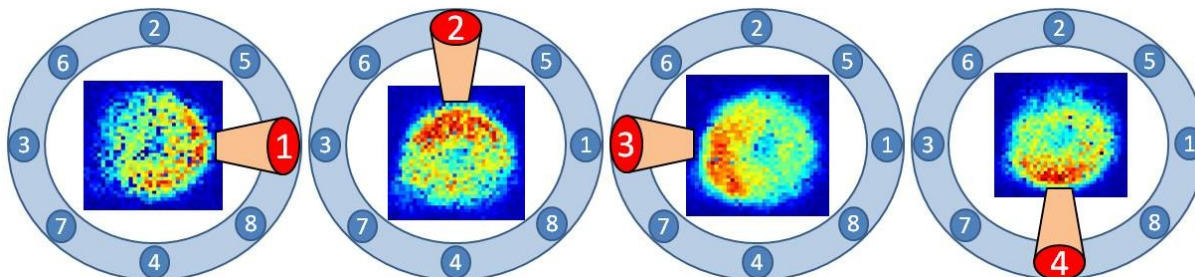


Figure 1. Raw fluorescence maps of oxygen derived from detectors 1, 2, 3 and 4. The red pixels correspond to high fluorescence intensity.

2.4. AFM and fluorescence elemental maps alignment

To register the raw elemental maps, obtained as described above, with the AFM maps Figure 2A, which has a different spatial resolution with respect to the first ones, we developed an automated operator independent alignment method. An accurate registration requires to align images with the same contrast and as much as possible with high signal to noise ratio. To this purpose we used as reference images the fluorescence raw maps (Figure 2B) of the sum of the eight detectors. Fluorescence raw maps were obtained by the program PyMCA as the sum of all the channels of the spectrum acquired at each scanning step. AFM was registered onto fluorescence raw maps using the images registration software FLIRT (<http://fsl.fmrib.ox.ac.uk/fsl/flirt/>) using a transformation with 6 degrees of freedom (1 rotation, 2 translation, 2 scale, 1 skew i.e. oblique deformation). Registered images were then re-sampled interpolating with a tri-linear function. Figure 2C shows the AFM map after registration.

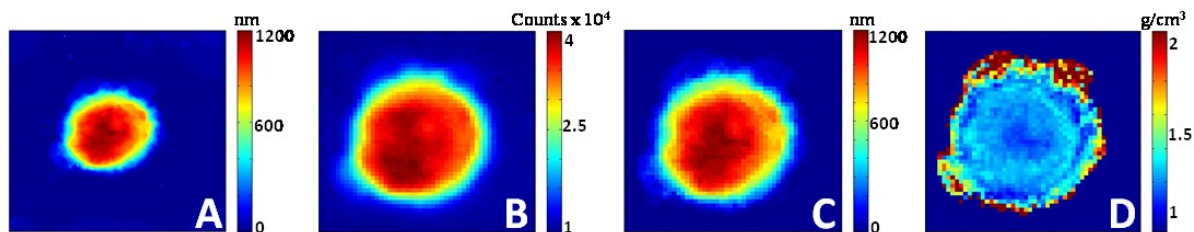


Figure 2. Panel A. AFM map. Panel B. Fluorescence raw map. Panel C. AFM registered onto fluorescence raw map. Panel D. Density map

2.5. XRFM self-absorption correction

Having a beam of energy E_0 and intensity I_0 incident at an angle α on the sample, at the depth z the intensity $I(z)$ is reduced to:

$$I(z) = I_0 e^{-\mu_m(E_0) \cdot \rho \cdot z \cdot \text{cosec}(\alpha)} \quad (1)$$

where $\mu_m(E_0) = \sum_i w(i) \mu_m(i)(E_0)$ is the mass absorption coefficient at the energy E_0 of the sample composed of elements i , $\mu_m(i)$ and $w(i)$ are the mass absorption coefficient and the mass fraction of element i respectively, and ρ is the sample density. In the infinitesimal sample volume $dV = Sdz$ at this depth, a number of atoms will be ionized and will give rise to the emission of fluorescent radiation with energy E_i . For an accurate assessment of elemental map derived from XRFM, the self-absorption in the sample must be taken into account using this equation:

$$A(i) = \int_0^d \exp\{-[\mu_m(E_0) \text{cosec}(\alpha) + \mu_m(E_i) \text{cosec}(\beta)] \rho z\} dz \quad (2)$$

Where $A(i)$ is the correction map for the element i , d the sample thickness, and β the exit angle of the fluorescence radiation collected by the detector. In this work we used tabulated values for $\mu_m(i)$ and approximate values, taken by literature, of $w(i)$ for major cell components (C, N and O) in dehydrated cells: ($w(O)$: 0.57, $w(N)$: 0.14, $w(C)$: 0.28) [8]. In equations (1) and (2) ρ is the density of the sample assessed using the relation $\rho = \mu_l / \mu_m(E_0)$ where μ_l is the linear absorption coefficient. We experimentally determined μ_l from the transmitted intensity T , which was measured at each scanning step, simultaneously to fluorescence detection. T is related to μ_l and to thickness t through the simple relation: $T = \exp(-\mu_l t)$. We calculated the μ_l map simply inverting the above expression: $\mu_l = (1/t) * \ln(1/T)$, and using the thickness map measured by the AFM previously registered onto transmission and fluorescence space. Figure 2D shows the density map obtained by measuring the transmission intensity. For an accurate evaluation of elemental distribution, the fluorescence maps must be corrected for self-absorption. To this purpose we elaborated an ad-hoc program, as much as possible automatic and operator independent, considering for each measuring point the path through the cell that the exiting fluorescence had to traverse in its way towards the detector. Each pixel of the AFM registered map was divided into small voxels of thickness dz . For each voxel the self-absorption from total path into the cell matrix has been calculated as shown in Figure 3. Then the contribution to fluorescence of each voxel has been summed up to obtain a correction map for each element according to equation 2. This procedure has been repeated for each detector. Figure 4 shows the final result,

comparing the uncorrected fluorescence maps with the corrected ones. It must be underlined that a strong contribution to the nitrogen fluorescence comes from the substrate, composed of Si_3N_4 . In the uncorrected map, the N fluorescence is indeed stronger outside the cell than in the cell, due to the absorption within the cell itself. We therefore subtracted the contribution from the substrate, corrected for absorption into the cell, to the total N fluorescence intensity, and then we applied the correction for self-absorption.

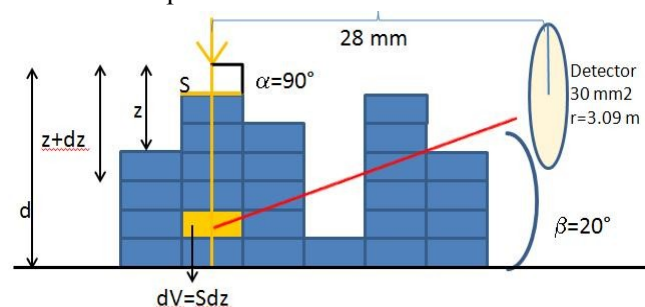


Figure 3. Scheme for the self-absorption correction in one voxel. The path which the fluorescence excited in the given voxel (in yellow) has to traverse through the cell, is calculated pixel by pixel taking into account the morphology measured by AFM.

3. Conclusions

In this work we have demonstrated that it is possible to assess the distribution of the major cell components, together with light metal elements, with XRFM, and provided that correction for self-absorption is a necessary requisite. We developed an ad-hoc analysis program for merging the morphology information obtained using AFM and STXM with XRFM. This procedure is a crucial preliminary step for the quantitative determination of element distribution and concentration.

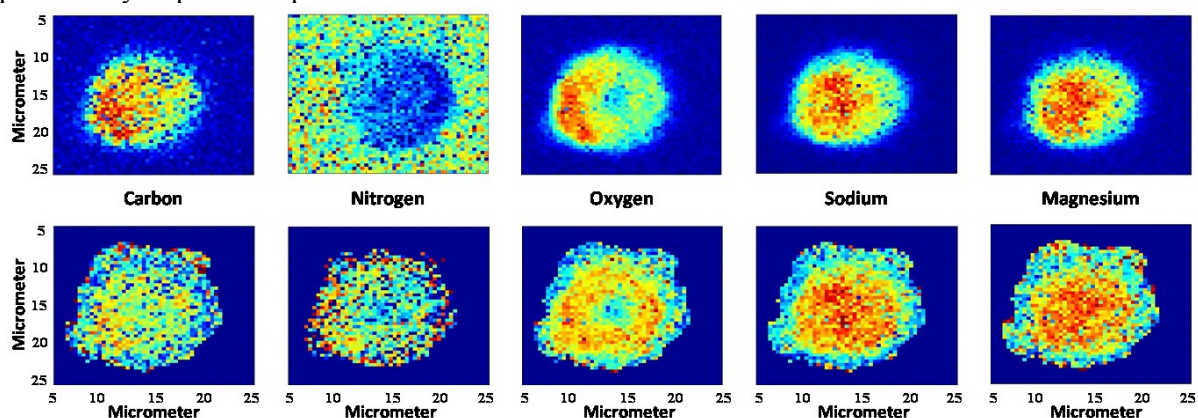


Figure 4. Uncorrected (top) and corrected (bottom) maps of C, N, O, Na and Mg.

References

- [1] Bohic S, Simionovici A, Snigirev A, Ortega R, Devès G, Heymann D and Schroer C G 2001 *Appl. Phys. Lett.* **78** 3544–46
- [2] Ortega R, Bresson C, Fraysse A, Sandre C, Devès G, Gombert C, Tabarant M, Bleuet P, Sez nec H, Simionovici A, Moretto P and Moulin C 2009 *Toxicol. Lett.* **188** 26–32
- [3] De Jonge M D, Holzner C, Baines S C, Twining B S, Ignatyev K, Diaz J, Howard D L, Legnini D, Miceli A, McNulty I, Jacobsen C J, and Vogt S., 2010 *PNAS*, **107** 15676-15680
- [4] Lagomarsino S, Iotti S, Farruggia G, Cedola A, Trapani V, Fratini M, Bukreeva I, Notargiacomo A, Mastrototaro L, Marraccini C, Sorrentino A, McNulty I, Vogt S, Legnini D, Kim S, Gianoncelli A, Maier J A M and Wolf F I 2011 *Spectrochim Acta B* **66**, 834–40
- [5] Gianoncelli A, Kaulich B, Alberti R, Klatka T, Longoni A, de Marco A, Marcello A and Kiskinova M 2009 *Nuclear Instr Meth Phys Res A* **608** 195-8
- [6] R. Hartmann, K.H. Stephan, L. Struder, *Nucl. Instr. and Meth. A* 439 (2–3) (2000) 216.
- [7] Solé V A, Papillon E, Cotte M, Walter P H and Susini J 2007 *Spectrochim Acta B* **62** 63-8
- [8] Heldal M, Norland S and Tumyr O 1985 *Appl Environ Microbiol* **50** 1251-57